

Supporting Information

Preferential vapor nucleation on hierarchical tapered nanowire bunches

*Bingang Du, Yaqi Cheng, Siyan Yang, Wei Xu, Zhong Lan, Rongfu Wen, Xuehu Ma**

State Key Laboratory of Fine Chemicals, Liaoning Key Laboratory of Clean Utilization of Chemical Resources, Institute of Chemical Engineering, Dalian University of Technology, Dalian 116024, PR China

*Corresponding Author E-mail: xuehuma@dlut.edu.cn

Table of contents

S1. Microscale observations of dropwise condensation	S2
S2. Chemical compositions of nanowire bunches	S2
S3. Theoretical analyses of the nucleation energy barrier	S3
S4. ESEM Setup.....	S7
S5. The statistic of nucleation positions	S8
Reference	S9

S1. Microscale observations of dropwise condensation

Video S1. Observation of nucleation when the sample is placed with a tilt angle of $\sim 45^\circ$. The field of view is $51\ \mu\text{m} \times 59\ \mu\text{m}$.

Video S2. Observation of nucleation when the sample is horizontally placed. The field of view is $84\ \mu\text{m} \times 73\ \mu\text{m}$.

Video S3. Observation of nucleation at a large view field. The field of view is $145\ \mu\text{m} \times 124\ \mu\text{m}$.

S2. Chemical compositions of nanowire bunches

Chemical compositions of the as-prepared hierarchical nanowire bunches are analyzed by energy-dispersive x-ray spectroscopy (EDS) under SEM. Figure S1a shows the elemental mapping of the whole area in the SEM image. The result indicates that the S element, which represents the hydrophobic layer ($\text{C}_{18}\text{H}_{38}\text{S}$), can be detected in all the regions, including the top and the sidewall of nanowire bunches. The content of the detected S element on the sidewall is lower than the top of the nanowire bunch in Figure S1a. We speculate that the majority of S element on the sidewall is not detected as the sidewall is not in the same plane with the top surface. To confirm the speculation, we reduce the scan area and characterize the local regions of the sidewall. As expected, more S element is detected around the top of the nanowire bunch and the lower part of the sidewall, as shown in Figure S1b and S1c. During the condensation process, preferential nucleation occurs around the top of nanowire bunches, where there exists hydrophobic layer. Above all, the EDS results show that the hydrophobic layer is deposited on the nanowire arrays homogeneously, and chemical compositions do not govern the preferential nucleation phenomenon.

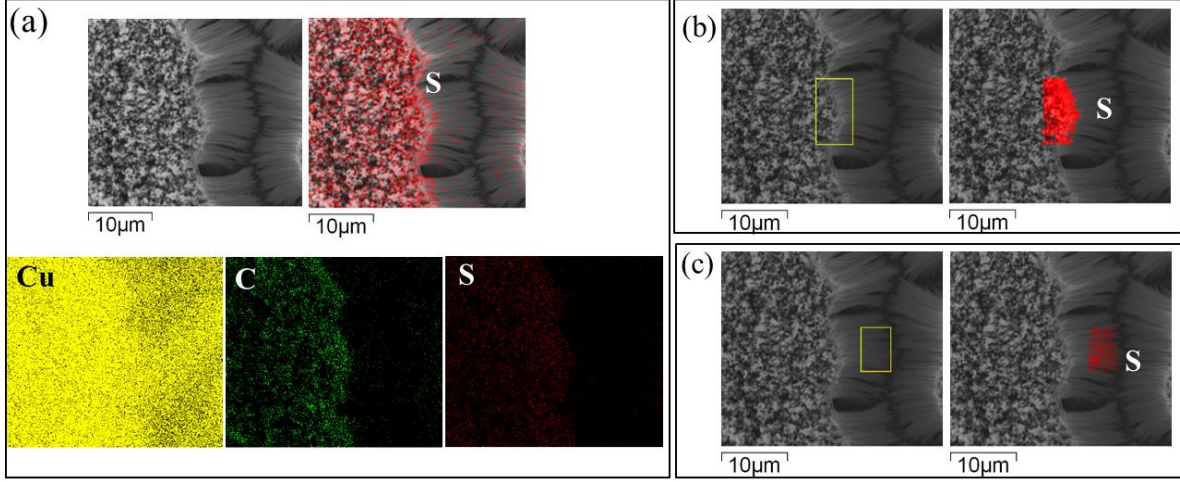


Figure S1. Elemental mapping of as-prepared hierarchical superhydrophobic nanowire bunches. (a) Elemental mapping of the whole area in the SEM image. (b) Elemental mapping of the region around the top of the nanowire bunch (c) Elemental mapping of the bottom of the sidewall of the nanowire bunch.

S3. Theoretical analyses of the nucleation energy barrier

Using the classical nucleation theory, the capillary approximation and Young' equation, the nucleation free energy barrier of the critical nucleus ΔG can be expressed as:¹⁻²

$$\Delta G = -\frac{\rho V_{\text{drop}}}{M} N_A k_B T \ln S + \sigma_{\text{lv}} (S_{\text{lv}} - S_{\text{ls}} \cos \theta) \quad (\text{S1})$$

Where M , ρ , and σ_{lv} are the molecular mass of the water, density, surface tension of water. N_A and k_B are the Avogadro's number and Boltzmann constant. T , S , and θ represent the temperature, the supersaturation, and the contact angle. S_{lv} and S_{ls} are the liquid-vapor interfacial area and liquid-solid contact area.

The nucleation droplet radius r_e is:²

$$r_e = \frac{2\sigma_{\text{lv}} T_v}{\rho h_{\text{lv}} \Delta T} \quad (\text{S2})$$

Where T_v , ΔT , and h_{fg} are the vapor temperature, surface subcooling, and latent heat.

Then we analyze the solid-liquid contact characteristics at different regions of a nanowire bunch, thus calculating S_{lv} and S_{ls} , as shown in Figure S2, S3. The curvature radius in all the calculation is equal to r_e (Equation S3). Figure S2a shows the initial droplet on the top of a nanowire. The related parameters can be calculated from the geometries.

$$r = r_e \quad (S3)$$

$$V_{\text{drop}} = \frac{\pi r^3}{3} (1 - \cos \theta)^2 (2 + \cos \theta) \quad (S4)$$

$$S_{lv} = 2\pi r^2 (1 - \cos \theta) \quad (S5)$$

$$S_{ls} = \pi r^2 \sin^2 \theta \quad (S6)$$

By substituting Equations S2-S6 into Equation S1, the energy barrier for nucleation on the top of a nanowire ΔG_1 can be obtained:

$$\Delta G_1 = \frac{1}{3} \pi r^2 \sigma_{lv} (2 - 3 \cos \theta + \cos^3 \theta) \quad (S7)$$

Figure S2b shows the initial droplet on the nanogrooves of nano-steps. According to the model proposed by Jin et al.,³ the related parameters can be calculated as:

$$V_{\text{drop}} = \frac{1}{3} r^3 [\cos \theta \sin^2 \theta \sin \beta - \cos \theta (3 - \cos^2 \theta) \beta + 4 \sin^{-1}(\sin \frac{\beta}{2} \sin \frac{\alpha}{2})] \quad (S8)$$

$$S_{lv} = r^2 [4 \sin^{-1}(\sin \frac{\beta}{2} \sin \frac{\alpha}{2}) - 2 \beta \cos \theta] \quad (S9)$$

$$S_{ls} = S_{sv} = r^2 \sin^2 \theta (\sin \beta - \beta) \quad (S10)$$

The nucleation energy barrier for nucleation on nano-steps ΔG_2 can be calculated by substituting Equations S8-S10 into Equation S1:

$$\Delta G_2 = \frac{1}{3} r^2 \sigma_{lv} \left[\cos \theta \sin^2 \theta \sin \beta - \cos \theta (3 - \sin^2 \theta) \beta + 4 \sin^{-1}(\sin \frac{\beta}{2} \sin \frac{a}{2}) \right] \quad (S11)$$

$$\cos \frac{\beta}{2} = \cot \theta \cot \frac{\alpha}{2} \quad (\text{S12})$$

Where α is the crosssectional angle of nano-grooves in the nano-steps.

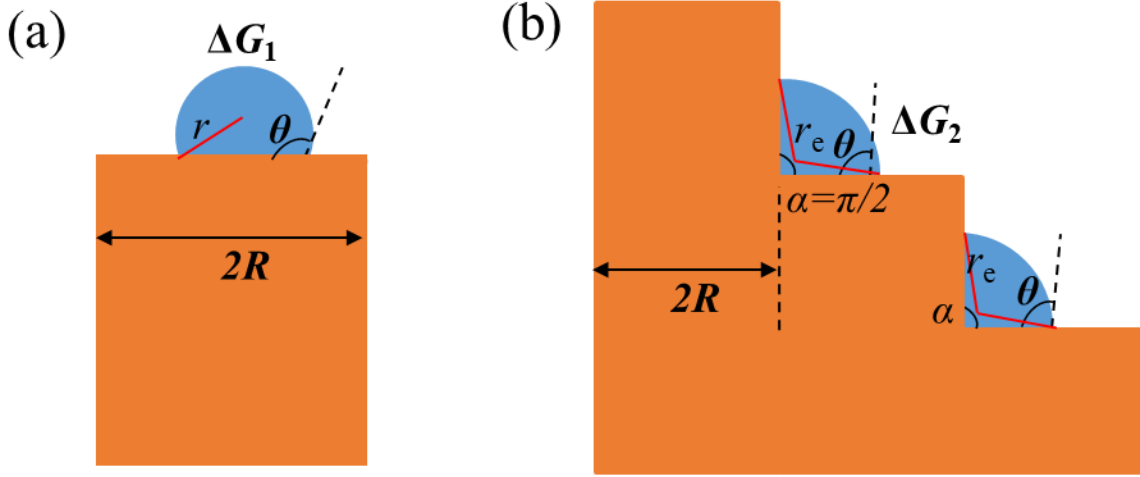


Figure S2. Sketch showing nucleation occurs (a) on the top of nanowires and (b) on the nano-steps around the top of nanowire bunches.

Figure S3 shows initial droplets on the gaps between two nanowires. The related parameters can also be calculated from the geometry:

$$d_1 = \sqrt{R^2 + r^2 - 2Rr \cos \theta_1} \quad (\text{S13})$$

$$d_2 = \sqrt{R^2 + r^2 - 2Rr \cos \theta_2} \quad (\text{S14})$$

$$g_1 = \sqrt{\left(\frac{R}{r}\right)^2 + 1 - 2\frac{R}{r} \cos \theta_1} \quad (\text{S15})$$

$$g_2 = \sqrt{\left(\frac{R}{r}\right)^2 + 1 - 2\frac{R}{r} \cos \theta_2} \quad (\text{S16})$$

$$V_{\text{drop}} = \frac{1}{3} \pi r^3 (3 \cos \psi_1 - \cos^3 \psi_1) - \frac{1}{3} \pi R^3 (2 - 3 \cos \varphi_1 + \cos^3 \varphi_1) + \frac{1}{3} \pi r^3 (3 \cos \psi_2 - \cos^3 \psi_2) - \frac{1}{3} \pi R^3 (2 - 3 \cos \varphi_2 + \cos^3 \varphi_2) \quad (\text{S17})$$

$$S_{\text{lv}} = 2\pi r^2 \cos \psi_1 + 2\pi r^2 \cos \psi_2 \quad (\text{S18})$$

$$S_{\text{ls}}=S_{\text{sv}}=2\pi R^2(2-\cos\varphi_1-\cos\varphi_2) \quad (\text{S19})$$

$$\cos\varphi_1=(R-r\cos\theta_1)/d_1 \quad (\text{S20})$$

$$\cos\psi_1=(r-R\cos\theta_1)/d_1 \quad (\text{S21})$$

$$\cos\varphi_2=(R-r\cos\theta_2)/d_2 \quad (\text{S22})$$

$$\cos\psi_2=(r-R\cos\theta_2)/d_2 \quad (\text{S23})$$

$$l_1=2(\sqrt{R^2+r^2-2Rr\cos\theta}-R) \quad (\text{S24})$$

$$l_2=\sqrt{R^2+r^2-2Rr\cos\theta}-R+r \quad (\text{S25})$$

The energy barrier for nucleation in the gaps between two nanowires ΔG_3 can be deduced by substituting Equations S13-S25 into Equation S1:

$$\begin{aligned} \Delta G_3 = & \frac{2}{3}\pi r^2\sigma_{\text{lv}} \left[\left(\frac{1-\frac{R}{r}\cos\theta_1}{g_1} \right)^3 + \left(\frac{1-\frac{R}{r}\cos\theta_2}{g_2} \right)^3 + \left(\frac{R}{r} \right)^3 \left(4-3\frac{\frac{R}{r}-\cos\theta_1}{g_1}-3\frac{\frac{R}{r}-\cos\theta_2}{g_2} \right. \right. \\ & \left. \left. + \left(\frac{\frac{R}{r}-\cos\theta_1}{g_1} \right)^3 + \left(\frac{\frac{R}{r}-\cos\theta_2}{g_2} \right)^3 \right) \right] \\ & + \frac{3}{2} \left(\frac{R}{r} \right)^2 \left(\frac{\frac{R}{r}-\cos\theta_1}{g_1} + \frac{\frac{R}{r}-\cos\theta_2}{g_2} - 2 \right) \cos\theta_1 \end{aligned} \quad (\text{S26})$$

Where θ_1 and θ_2 are the droplet contact angles on two neighboring nanowires. When the nanowire interspace $l \leq l_1$, the solid-liquid interfacial area and liquid-vapor interfacial area are constant, as shown in Figure S3a and S3b. The contact angles are expressed as:

$$\theta_1 = \theta_2 = \theta \quad (\text{S27})$$

Where θ is the contact angle of plain hydrophobic surface. When $l \geq l_2$, the initial droplet forms on the individual nanowire:

$$\theta_1 = \theta \quad (\text{S28})$$

$$\theta_2 = 180^\circ \quad (\text{S29})$$

When $l_2 < l < l_1$, the initial droplet forms between two nanowires,

$$\theta_1 = \theta \quad (\text{S30})$$

$$\cos \theta_2 = \frac{R^2 + r^2 - (l - d_1 + 2R)^2}{2Rr} \quad (\text{S31})$$

By substituting Equation S27, Equations S28-S29 or Equations S30-S31 into Equation S26, the relationship between the nucleation energy barrier and the nanowire interspace l can be obtained (Figure 5h).

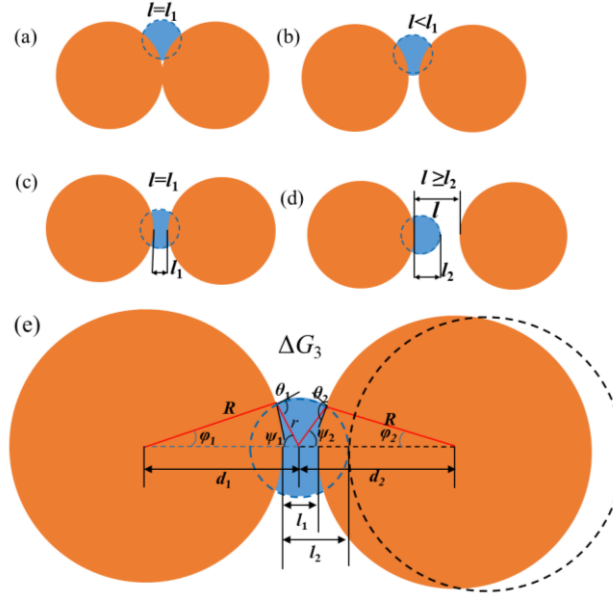


Figure S3. Sketch showing the solid-liquid contact characteristics (a-c) on the gaps between nanowires when the nanowire interspace is small, (d) on an individual nanowire when the nanowire interspace is larger than l_2 . (e) The relative parameters when calculating nucleation barriers.

S4. ESEM Setup

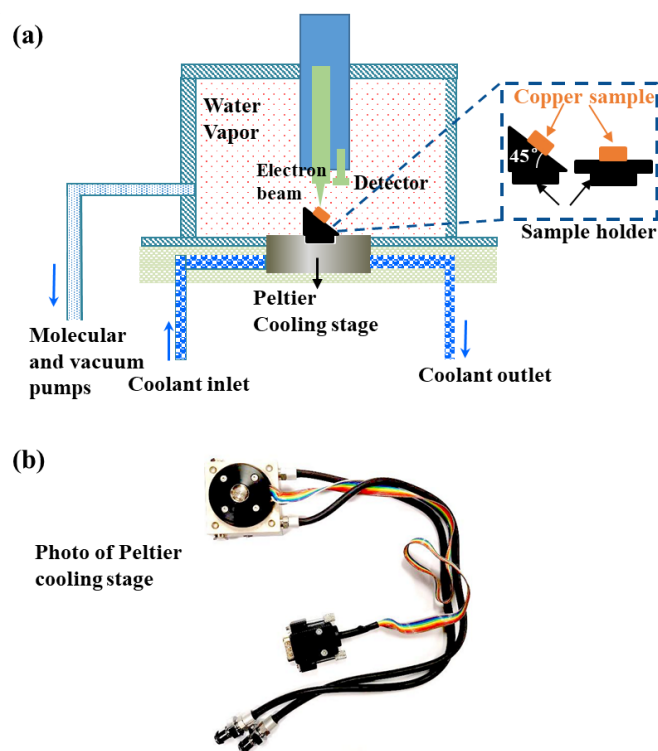


Figure S4. Schematic of the experimental setup (a) and the photo of Peltier cooler (b) in ESEM.

S5. The statistic of nucleation positions

We further study the nucleation positions at different sections of the hierarchical surface, as shown in Figure S5. (Figure S5a is corresponding to Video S3). The size of each section is $147\ \mu\text{m} \times 127\ \mu\text{m}$. Seventy-two nucleation events are observed and 10 % of nucleation events occur at the bottom or sidewall of nanowire bunches.

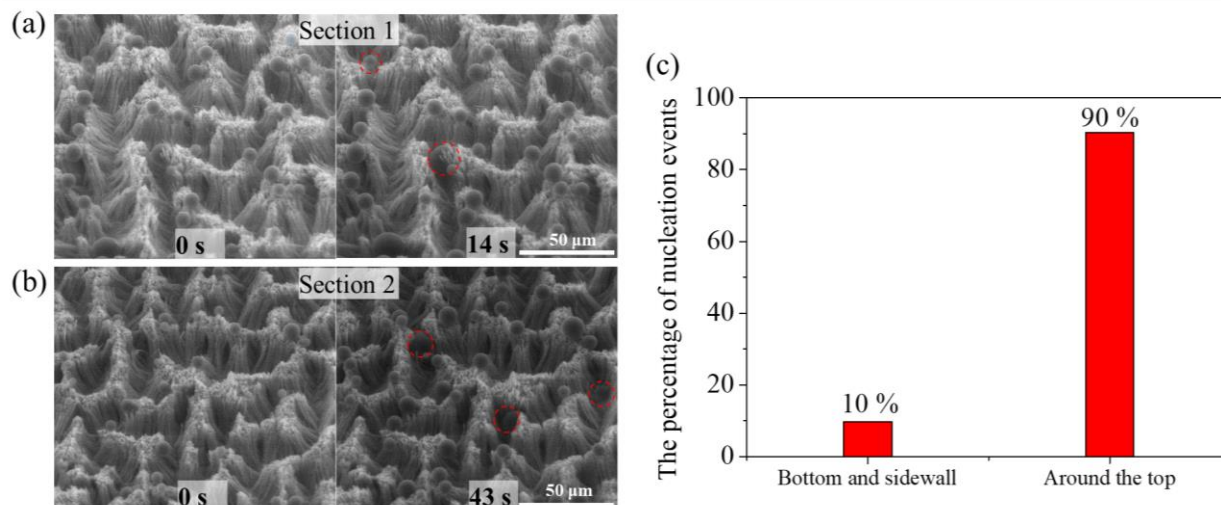


Figure S5. Images showing droplet nucleation characteristics on (a) section 1 and (b) section 2 of the hierarchical surface. (c) The statistic of nucleation events on different regions of nanowire bunches.

Reference

- (1) Carey, V. P., Liquid vapor phase change phenomena: an introduction to the thermophysics of vaporization and condensation processes in heat transfer equipment. CRC Press: 2020.
- (2) Xu, W.; Lan, Z.; Peng, B.; Wen, R.; Ma, X., Heterogeneous nucleation capability of conical microstructures for water droplets. *RSC Adv.* **2015**, 5 (2), 812-818.
- (3) Jin, Y.; Qamar, A.; Shi, Y.; Wang, P., Preferential water condensation on superhydrophobic nano-cones array. *Appl. Phys. Lett.* **2018**, 113 (21), 211601.